Mid- to- late Holocene hydroclimatic changes on the Chinese Loess Plateau

Sun, Huiling; Bendle, James; Seki, Osamu; Zhou, Aifeng

DOI:
10.1007/s10933-018-0037-9

Journal of Paleolimnology

Mid- to- late Holocene hydroclimatic changes on the Chinese Loess Plateau: evidence from n-alkanes from the sediments of Tianchi Lake

--Manuscript Draft--

Manuscript Number:	JOPL-D-17-00035R4
Full Title:	Mid- to- late Holocene hydroclimatic changes on the Chinese Loess Plateau: evidence from n-alkanes from the sediments of Tianchi Lake
Article Type:	Papers
Keywords:	n-Alkanes · Paq · Lake level · Mid-late Holocene · Loess Plateau
Corresponding Author:	Aifeng Zhou Lanzhou University Lanzhou, Gansu CHINA
Corresponding Author Secondary Information:	
Corresponding Author's Institution:	Lanzhou University
Corresponding Author's Secondary Institution:	
First Author:	Huiling Sun
First Author Secondary Information:	
Order of Authors:	Huiling Sun
	James Bendle
	Osamu Seki
	Aifeng Zhou
Order of Authors Secondary Information:	
Funding Information:	National Natural Science Foundation of China (41761044) — Dr. Huiling Sun
	National Natural Science Foundation of China (41771208) — Dr. Aifeng Zhou
	China Scholarship Council (2009618032) — Dr. Huiling Sun
Abstract:	We have reconstructed the history of mid-late Holocene paleohydrological changes in the Chinese Loess Plateau using n-alkane data from a sediment core in Tianchi Lake. We used Paq (the proportion of aquatic macrophytes to the total plant community) to reflect changes in lake water level, with a higher abundance of submerged macrophytes indicating a lower water level and vice versa. The Paq -based hydrological reconstruction agrees with various other lines of evidence, including ACL (average chain length), CPI (carbon preference index), C/N ratio and the n-alkane molecular distribution of the sediments in Tianchi Lake. The results reveal that the lake water level was relatively high during 5.7 to 3.2 ka BP, and decreased gradually thereafter. Our paleohydrological reconstruction is consistent with existing paleoclimate reconstructions from the Loess Plateau, which suggest a humid mid-Holocene, but is asynchronous with paleoclimatic records from central China which indicate an arid mid-Holocene. Overall, our results confirm that the intensity of the rainfall delivered by the EASM (East Asian summer monsoon) is an important factor in affecting paleohydrological changes in the region and can be considered as further evidence for the development of a spatially asynchronous "northern China drought and southern China flood" precipitation pattern during the Holocene.
Suggested Reviewers:	Cheng Zhao Professor, Nanjing Institute of Geography and Limnology Chinese Academy of

	Sciences czhao@niglas.ac.cn
	Zhonghui Liu Professor, University of Hong Kong zhliu@hku.hk
	James Russell associate professor, Brown University James_Russell@brown.edu
Response to Reviewers:	Dear Professor Whitmore, Thanks you so much for your corrected my manuscript. I accepted all the corrections and “accept all changes”. Best regards! Sincerely, Aifeng

Mid- to- late Holocene hydroclimatic changes on the Chinese Loess Plateau: evidence from *n*-alkanes from the sediments of Tianchi Lake

Huiling Sun[a] · James Bendle[b] · Osamu Seki[c] · Aifeng Zhou[d]*

a. *Key Laboratory of Plateau Lake Ecology and Global Change, College of Tourism and Geography, Yunnan Normal University, Kunming, 650500, China*

b. *School of Geography, Earth and Environmental Sciences, University of Birmingham, Edgbaston, Birmingham, B15 2TT, UK*

c. *Institute of Low Temperature Science, Hokkaido University, N19W8, Kita-ku, Sapporo, 060-0819, Japan*

d. *Key Laboratory of Western China's Environmental Systems（Ministry of Education), College of Earth and Environmental Sciences, Lanzhou University, Lanzhou, 730000, China*

***** Corresponding Author: Aifeng Zhou (zhouaf@lzu.edu.cn)

Address: 222 Tianshui South Road, Lanzhou, Gansu, P.R.China. 730000

Phone: (+86)13893612602

Key words

n-Alkanes · P_{aq} · Lake level · Mid-late Holocene · Loess Plateau

Abstract

We have reconstructed the history of mid-late Holocene paleohydrological changes in the Chinese Loess Plateau using *n*-alkane data from a sediment core in Tianchi Lake. We used P_{aq} (the proportion of aquatic macrophytes to the total plant community) to reflect changes in lake water level, with a higher abundance of submerged macrophytes indicating a lower water level and vice versa. The P_{aq} -based hydrological reconstruction agrees with various other lines of evidence, including ACL (average chain length), CPI (carbon preference index), C/N ratio and the *n*-alkane molecular distribution of the sediments in Tianchi Lake. The results reveal that the lake water level was relatively high during 5.7 to 3.2 ka BP, and decreased gradually thereafter. Our paleohydrological reconstruction is consistent with existing paleoclimate reconstructions from the Loess Plateau, which suggest a humid mid-Holocene, but is asynchronous with paleoclimatic records from central China which indicate an arid mid-Holocene. Overall, our results confirm that the intensity of the rainfall delivered by the EASM (East Asian summer monsoon) is an important factor in affecting paleohydrological changes in the region and can be considered as further evidence for the development of a spatially asynchronous “northern China drought and southern China flood” precipitation pattern during the Holocene.

Introduction

Climatic and environmental changes in the Chinese Loess Plateau are mainly controlled by the EASM, which directly affects almost all aspects of the hydrology and ecology of East Asia (Clift and Plumb 2008). An increase in EASM intensity would be expected to result in a northward movement of the rainfall belt in China and a corresponding rainfall increase in the Loess Plateau (Chen et al. 2008). Many regional paleoclimatic records have been produced from this semi-arid, monsoon marginal zone (Zhao et al. 2010; Dong et al. 2012; Liu and Feng 2012; Lu et al. 2013; Qiang et al. 2013). However, regional high-resolution paleohydrological reconstructions are extremely limited because proxies or archives that record ancient hydrological conditions, with good age control, are scarce on the Loess Plateau. A humid mid-Holocene has been proposed based on a pollen-based record (Chen et al. 2015a) and a hydrogen isotope reconstruction of long-chain *n*-alkanes (Rao et al. 2016) from Gonghai Lake, one of the few natural lakes on the Loess Plateau. Their paleohydrological reconstruction is inconsistent with records from the core monsoon-controlled regions of central China. It shows an arid interval from 7.0-3.0 ka BP (Xie et al. 2013; Zhu et al. 2017). Therefore, more high-resolution lacustrine reconstructions of hydroclimatic variations during the mid-late Holocene are needed to explore the underlying mechanism of this asynchronous hydroclimatic variability. Here, a high-resolution lacustrine record based on *n*-alkanes of sediments from Tianchi Lake on the Loess Plateau will be discussed.

n-Alkanes preserved in lake sediments can be used to infer variations in the composition and origin of organic inputs to the lacustrine environment, because they are widely preserved in various environmental contexts, such as plants, soils and lacustrine sediments, and can resist degradation actions (Meyers 1997). In particular the Average Chain Length (ACL) (Poynter and Eglinton 1990), Carbon Preference Index (CPI) (Meyers and Ishiwatari 1993), and P_{aq} (Ficken et al. 2000) *n*-alkane indices, have been widely used in paleoenvironmental research (Nichols et al. 2006; He et al. 2014). In general, terrestrial plants and emergent macrophytes are typically dominated by the long-chain length homologues (C_{27}-C_{33}) (Ficken et al. 2000; Gao et al. 2011), while submerged and floating-leaved macrophytes mainly produce C_{23} and C_{25} *n*-alkanes (Ficken et al. 2000), and short chain ones are produced by algae and bacteria (Cranwell et al. 1987). Consequently, higher ACL and CPI are commonly considered to be predominantly produced by terrestrial plants. A higher P_{aq} may result from an increase in submerged macrophytes in combination with a recession of the terrestrial plants around the lake. Moreover, the biomass of submerged macrophytes is related to the variation of the water table (Wagner and Falter 2002; Liu et al. 2015), and lake level fluctuations have the potential to simultaneously constrain the spatial distribution and the biomass of submerged macrophytes in a lake (Duarte and Kalf 1986; Hudon 1997; Middelboe and Markager 1997). Howerver, Aichner et al. (2010) and Liu et al. (2015) found that higher amounts of long chain *n*-alkanes can be produced by submerged macrophytes in several lakes. Therefore, it is necessary to understand the extent to which long chain *n*-alkanes in lacustrine sediments are

influenced by terrestrial plants and submerged macrophytes in a study lake when reconstructing the paleoenvironments.

In this study, we first define the potential sources and the contributions from the various plants (e.g. terrigenous plants vs. submerged macrophytes) in Tianchi Lake. Second, we give an interpretation of the proxies (P_{aq}, ACL, CPI of *n*-alkanes, and C/N), especially P_{aq} as an effective indicator of lake level changes in Tianchi Lake. Additionally, we seek to compare regional climate reconstructions with those from Tianchi Lake and other nearby sites to confirm a spatially asynchronous hydroclimatic variability occurred in China during the Holocene.

Study site

Tianchi Lake (lat. 35º15’55’’N, long. 106º18’43’’E, elevation 2430 m a.s.l.) is a small freshwater alpine lake located in the Liupan Mountains, southwestern Loess Plateau, northwest China (Fig. 1a). The length of the lake from east to west is 250 m and the width is 120 m. The maximum water depth is 8.2 m, and the lake covers an area of 2×10^4 m^2 (Fig. 1b). The lake receives no surface run off, and it is fed by meteoric water and groundwater recharge. There is no apparent surface outflow, except for a possible transient outflow in the western part of the lake basin, which is possibly active during the rainy season. The mean annual temperature is 8.2 °C and mean annual precipitation is 677 mm based on data from the nearest meteorological station (Liupan Mountain station, at 2845 m a.s.l.). Most of the precipitation occurs as

rainfall during summer, accounting for nearly 72.2% of the annual total. The vegetation of the upland slopes of the lake is dominated by shrubs and steppe. Grassy steppe with sparse shrub covers the north slopes, and shrubs dominate the south slopes (Zhao et al. 2010). Emergent (*Phragmites australis* (Cav.) Trin. ex Steud) and submerged (*Potamogeton* sp. and *Chara* sp.) macrophytes are widely distributed in the shallow areas of the lake (Fig. 1d), but floating-leaved macrophytes are absent, based on our field observations in 2010.

Materials and methods

Field sampling

Two parallel sediment cores of lengths 11.2 m (GSA07-1) and 10.4 m (GSB07-1) were collected using a UWITEC piston corer system (6 cm in diameter) from the lake center in 2007 (Fig. 1b). The lithology of core GSB07-1 consisted of alternating brown-colored sandy clay and grey-brownish clay between 1040-746 cm, and grey-brownish clay above 746 cm. The sediments are characterized by 1 to 2-mm-thick organic detritus-rich laminations (Fig. 1c), which yielded abundant terrestrial macrofossils for radiocarbon dating. Fifty-six down-core sedimentary samples were taken at 15-cm intervals throughout core GSB07-1. Additionally, we collected six surface soil samples, three surface lake sediments, nine dominant terrestrial plant samples (*Cedrus* sp., *Larix* sp., *Abies* sp., *Betula* sp., *Rosa* sp., *Rubus*

sp., *Salix* sp., *Berberis* sp. and *Artemisia* sp.), which surround the lake, and one emergent macrophyte (*P. australis*) and two submerged macrophytes (*Potamogeton* and *Chara*) within the lake for modern process study. All the above samples were carried out for TOC, TN analyses, and lipid extraction.

Laboratory analyses

Samples for TOC and TN measurements were pretreated with 10 ml of 10% HCl to remove carbonates, washed with distilled water until the pH was neutral, and then measured using a CE Model 440 Elemental Analyzer. The C/N ratio was derived from the ratio of TOC and TN. *n*-Alkanes were extracted based on methods described previously (Kawamura et al. 2003) in G-MOL lab of the University of Glasgow. Briefly, 2-10 g of freeze-dried, homogenized sediment were transferred to a test tube and hydrolyzed with 15 ml of 0.3 M KOH dissolved in 95:5 methanol/dichloromethane-extracted water. The samples were then hydrolyzed and centrifuged and the supernatant and pipetted into a round-bottomed flask. The sediment was then extracted three times with 10 ml dichloromethane/methanol (3:1) using ultrasonication. The extracts were combined and concentrated, using a rotary evaporator, under vacuum and then separated into neutral and acidic fractions using the methods of Kawamura (1995). The neutral fraction was further separated using silica gel column chromatography to get *n*-alkane fraction. Dried *n*-alkane fraction was redissolved in hexane and analyzed using a gas chromatograph (GC; Shimadzu

2010) with a flame ionization detector (FID) and hydrogen as carrier gas at constant pressure (190 kPa). Separation of the different compounds was achieved using an identical column (length: 60 m, diameter: 0.25 mm, film thickness: 0.25 μm, coating: 100 % dimethyl-polysiloxane). The gas chromatograph temperature program was set to increase from 50 -120 °C at 30 °C min^{-1}, then 120 -310 °C at 5 °C min^{-1}, with a final isothermal time of 20 min at 300 °C. Compound identification was confirmed by GC/MS (Shimadzu OP2010-Plus Mass Spectrometer (MS) interfaced with a Shimadzu 2010 GC) based on retention times and mass spectra.

The *n*-alkane proxies (equation (1) from Poynter and Eglinton (1990); equation (2) from Marzi et al. (1993); and equation (3) from Ficken et al. (2000) were calculated as follows:

$$ACL=(19*C_{19}+20*C_{20}+21*C_{21}+\cdots+33*C_{33})/(C_{19}+C_{20}+C_{21}+\cdots+C_{33}) \quad (1)$$

$$CPI =7/8*(C_{19}+C_{21}+C_{23}+\cdots+C_{33})/(C_{20}+C_{22}+C_{24}+\cdots+C_{32}) \quad (2)$$

$$P_{aq} = (C_{23}+C_{25})/(C_{23}+C_{25}+C_{29}+C_{31}) \quad (3)$$

where C_i is the concentration of *n*-alkane of i number of carbon.

Age model

The chronology of core GSA07-1 used in this study mainly consists of 19 dates from Zhao et al. (2010) and 6 new dates (Table 1). All ^{14}C dates were measured in the AMS Dating Laboratory of Beijing University and are based on the leaves of terrestrial plants. The ages were calibrated to calendar years before present (AD 1950) using the

program CALIB Rev. 5.0.1 with the IntCal04 calibration data set (Reimer et al. 2004). The depths of characteristic laminations in cores GSA07-1 and core GSB07-1 are consistent. Therefore, the chronology of core GSB07-1 was calibrated based on the corresponding depths in GSA07-1 (Table 1). The chronology indicates that the age of core GSB07-1 spans the past 5720 years (Fig. 2). The average accumulation rate based on the age-depth model is about 1.85 mm a^{-1}.

Results

n-Alkane distributions and P_{aq} variations in modern vegetation

The P_{aq} index has been proposed as an indicator of the relative contributions of *n*-alkanes from submerged/floating aquatic plants versus those from emergent and terrestrial plants in the lake. Generally, P_{aq} <0.1 corresponds to terrestrial plants, 0.1-0.4 to emergent macrophytes, and 0.4-1.0 to submerged/floating macrophytes (Ficken et al. 2000). In this study, average P_{aq} values and *n*-alkane molecular distribution patterns vary considerably in the three types of plant material (terrestrial, and emergent and submerged macrophytes: Fig. 3a-c). Terrestrial plants (Fig. 3a), which have a lower average P_{aq} value (0.18), are dominated by the *n*-C_{31} homologue. Emergent macrophytes (Fig. 3b) growing in the near-shore environment are mainly dominated by the *n*-C_{27} homologue and have a higher P_{aq} value (0.65). In contrast, *n*-C_{23} is the dominant homologue in the submerged macrophytes (Fig. 3c) with a secondary peak at *n*-C_{25}. The average P_{aq} value of submerged macrophytes is 0.93. In

addition, a bimodal *n*-alkane distribution pattern with high abundances at *n*-C_{23} and *n*-C_{31} is observed in the surface sediments of Tianchi Lake which have an average P_{aq} value of 0.51 (Fig. 3d), indicating a specific mixture of inputs from terrestrial plants and submerged macrophytes. The distribution pattern for the surface soil has an overwhelming preponderance of the *n*-C_{31} homologue, and the average P_{aq} value of the surface soils is 0.25 (Fig. 3e).

n-Alkane proxies and C/N ratios in the down-core sediments

Time series of the various sedimentary parameters are illustrated in Fig. 4. The records span the last 5.7 ka BP. P_{aq} (Fig. 4a) ranges from 0.32 to 0.78 with a mean of 0.56. The average P_{aq} value is 0.46 during 5.7-3.2 ka BP, and 0.65 from 3.2 ka BP to the present. It is noteworthy that prior 3.2 ka BP most of the P_{aq} values are less than 0.52, while subsequently they are greater than 0.52. ACL ranges from 25 to 29 with a mean of 27.4 (Fig. 4b). The CPI values range from 1.7 to 8.8 with a mean of 5.2 over the last 5.7 ka BP (Fig. 4c). The C/N ratios (Fig. 4d) range from 9.5 to 26 with a mean of 15. The ACL, CPI, and C/N ratios exhibit similar patterns of variation, and they all exhibit an obvious shift at 3.2 ka BP, as do the P_{aq} values. The threshold values of ACL, CPI, and C/N ratios are almost the same as their average values.

Discussion

Sources of organic matter to the lake

The organic component of lake sediments represents a pool of organic matter derived from the decomposing detritus of aquatic plants growing in the littoral and marginal zone of the lake and from terrestrial plants growing in the catchment (Meyers and Ishiwatari 1993; Meyers 1997). Lacustrine sediment *n*-alkanes often have multiple sources, including terrestrial plants, aquatic macrophytes and lower organisms. Generally, *n*-alkane distributions of terrestrial and emergent plants tend to exhibit high proportions of the *n*-C_{31} homologue (Rielley et al. 1991; Ficken et al. 2000; Sachse et al. 2006), whereas those of submerged and floating plants are generally dominated by *n*-C_{23} and *n*-C_{25} homologues (Ficken et al. 2000; Gao et al. 2011; Seki et al. 2012). Therefore, *n*-alkanes can be used to identify local and regional sources of organic matter. However, recent studies have indicated that aquatic plants also make a large contribution to the long chain *n*-alkanes in lake sediments (Aichner et al. 2010; Liu et al. 2015; Liu and Liu 2016). For example, Liu et al. (2015) found that the long chain *n*-alkanes produced by submerged plants in Qinghai Lake had a significant influence on *n*-C_{27} and *n*-C_{29} alkanes in sediments. Even for the same submerged plant (*Potamogeton* sp.) from 16 Tibetan Plateau lakes, the distribution patterns of all the *n*-alkane homologs show obvious differences (Liu and Liu 2016). It is thus necessary to make a distinction between the various sources that contribute to the organic matter in given study area. At present, the two types of submerged macrophytes (*Potamogeton* and *Chara*) in Tianchi Lake are dominated by mid-chain

n-alkanes (*n*-C_{23} and *n*-C_{25}) (Fig. 3c). The average P_{aq} value is as high as 0.93. There is no evidence that they exhibit relatively high abundance of long chain *n*-alkanes as Liu and Liu (2016) described. The unimodal distribution pattern with the maxima at *n*-C_{31} alkanes and relatively low P_{aq} values of modern terrestrial plants (Fig. 3a) and surface soils (Fig. 3e) in Tianchi Lake, suggest again that *n*-C_{31} alkanes can be traced to terrestrial plant inputs and not to lake macrophytes. In addition, a bimodal molecular distribution pattern with major peaks at the *n*-C_{23} and *n*-C_{31} homologues in the surface lake sediments (Fig. 3d) probably represents a combination of inputs from submerged macrophytes (Fig. 3c) and terrestrial plants (Fig. 3a)/emergent (Fig. 3b). Our observations are consistent with those of previous studies (Cranwell 1984; Ficken et al. 2000; Gao et al. 2011; Street et al. 2013), which indicate that P_{aq} can be used to reflect the contribution from submerged macrophytes.

Interpretation of *n*-alkane indices

It has been demonstrated that the abundance of submerged macrophytes in lake is affected by irradiance and the littoral slope (Hudon 1997; Hudon et al. 2000; Cheruvelil and Soranno 2008). Thus, lake level has the potential to constrain the spatial distribution of submerged macrophytes via both a reduction in light intensity (Duarte and Kalf 1986; Middelboe and Markager 1997) and a change in the spatial extent of the littoral habitat (Hudon 1997). Hence, changes in the relative inputs of submerged macrophytes can potentially be ascribed to fluctuations in lake level. Most

of the submerged macrophytes in Tianchi Lake are distributed in a shallow area close to the shoreline and very few floating macrophytes can be observed (Fig. 1d). *Potamogeton* and *Chara* are the two dominant submerged species, which grow in a narrow zone down to a depth of ~1.2 m. A bathymetric survey of Tianchi Lake (Fig. 1b) reveals that the shoreline forms a narrow shelf from a depth of 0.5 m down to 2.8 m, followed by a steep slope that causes a decrease in the occurrence of submerged macrophytes. Assuming that the basic bathymetry of the basin has remained similar through time, the reductions in lake level would result in a relatively larger shelf area, which would produce an expansion of the shallow-water habitat for submerged macrophytes. Accordingly, the lower P_{aq} values in Tianchi Lake could be interpreted as reflecting less abundance of submerged macrophytes and the raising of lake level. On the other hand, the contribution from terrestrial plants can also exert an influence on P_{aq} values since the P_{aq} index is a proxy for evaluating the contribution of *n*-alkanes from submerged/floating aquatic plants relative to emergent and terrestrial plants (Ficken et al. 2000). During intervals of high rainfall and lake level, an increased contribution of terrestrial plant material delivered by increased catchment rain and runoff could lower P_{aq} values, and vice versa. This coincides with the findings of Liu and Liu (2016), which indicated a negative relationship between the P_{aq} value of surface lake sediments and the water level of Qinghai Lake.

As an important parameter of *n*-alkanes, the climate implications of ACL have been discussed a lot in the literature, but there is no unified agreement as to their interpretation because ACL often appears highly specific to regional or local

conditions (Ling et al. 2017). Furthermore, ACL can not be used to reconstruct temperature or precipitation change if the plant species or sedimentary environment in the catchment area underwent considerable change (in parallel with or forced by climatic variation) (Pu et al. 2010). CPI is another *n*-alkane index, which has been widely accepted as an indicator for terrestrial sources of sedimentary organic matter. Terrestrial plants have abundant long-chain *n*-alkanes, and show distinct odd-even predominance, thus their CPI is always greater than 5. On the contrary, CPI values of the aquatic plants and planktonic bacteria are considerably lower than those usually reported for terrestrial plant sourced *n*-alkanes (Cranwell 1987).

Reconstruction of the lake-level evolution

n-Alkane based records and C/N ratios from Tianchi Lake are presented in Fig. 4. Overall, there is an obvious shift at ~3.2 ka BP among the various proxies. During 5.7-3.2 ka BP, the ACL (Fig. 4b) and CPI (Fig. 4c) proxies show relatively high values in the core. CPI values almost greater than 5 and ACL values range from 27 to 29, likely indicate a predominance of terrestrial plant inputs to the lake basin. The results are supported by the higher C/N ratios (mean >15, with occasional values up to 26) (Fig. 4d) in this phase since the C/N ratios from terrestrial plants and emergent macrophytes can be as high as 20 (Lamb et al. 2004). On the other hand, relatively lower P_{aq} values (0.32 - 0.56) (Fig. 4a) and a contrary changing trend of P_{aq} with ACL, CPI, C/N ratios, suggest a recession of the submerged macrophytes growing in

Tianchi Lake. Based on interpretations discussed above, less abundance of submerged macrophytes input and more abundance of terrestrial plants input to the sediments are likely a response to relatively high lake levels during this phase in Tianchi Lake.

We interpret the increase in average P_{aq} values (0.51-0.78) and a decrease in ACL (25-27) and CPI (1.6-5.4) after 3.2 ka BP (Fig. 4a) as corresponding to an increase in the proportion of submerged and floating-leaved macrophytes, and a decrease in terrestrial inputs. Furthermore, the C/N ratios are generally low (<15) during this interval. In view of the absence of floating-leaved macrophytes in Tianchi Lake, based on our field observations, the increasing contribution from submerged macrophytes accordingly indicates a gradually falling lake level from 3.2 ka BP.

The variations in lake level inferred by the *n*-alkanes record is also supported by a shift in pollen assemblages from Tianchi Lake, which indicate that closed canopy forest was replaced by an open landscape at around 3.0 ka BP (Zhao et al. 2010). Another high-resolution pollen record from the Dadiwan peatland (Fig. 1a), 50 km southwest of Tianchi Lake on the Loess Plateau, also reveals a significant decrease in tree pollen frequencies at around 3.0 ka BP (An et al. 2003).

Asynchronous hydroclimatic variability

The P_{aq} record from Tianchi Lake reveals a transition from higher lake levels to lower lake levels after 3.2 ka BP, and thus wetter conditions during 5.7-3.2 ka BP and drier conditions after 3.2 ka BP (Fig. 5d). This accords with other paleoclimatic records

from the nearby Chinese Loess Plateau (Lu et al. 2013; Chen et al. 2015a; Liu et al. 2015; Rao et al. 2016). The pollen-based annual precipitation reconstruction from Tianchi Lake suggests a rapid precipitation decrease since ~3.3 ka BP (Fig. 5e; Chen et al. 2015a). Another pollen-based annual precipitation reconstruction from nearby Gonghai Lake (Fig. 5f) reveals a humid interval around 8-3 ka BP (Chen et al. 2015a). A recent study of palaeosol development as an indicator of the strength of the EASM (Wang et al. 2014) suggests a wet interval during 8.6-3.2 ka BP in the Chinese Loess Plateau. In addition, a TOC record from the Dadiwan peat profile also revealed a similar pattern of wet and dry episodes as at Tianchi Lake (Zhou et al. 1996; Huang et al. 2013). This evidence supports the contention that a moist climate was a widespread phenomenon on the Chinese Loess Plateau during the mid-Holocene. It is in accord with the gradually decreasing solar insolation (Fig. 5g). However, the paleohydrological conditions reconstructed from Dajiuhu peatland (Fig. 5c) in the middle reaches of the Yangtze River of central China are in contrast with these previous paleoclimatic records. Changes in the aerobic bacteria-derived hopanoid flux in Dajiuhu peatland (Fig. 5c) imply relatively arid conditions from 7.0-3.0 ka BP and relatively wet conditions from 3.0-1.0 ka BP (Xie et al. 2013; Huang et al. 2013; He et al. 2015). Another late-Holocene paleohydrological reconstruction based on sediment grain-size and *n*-alkane data from Longgan Lake in the middle and lower reaches of the Yangtze River (Xue et al. 2017), indicated drought conditions from 4 to 2.7 ka BP and a humid interval from 2.7 to 1.2 ka BP. In addition, the studies on the $\delta^{18}O$ (Fig. 5a) and the flux of soil-derived magnetic minerals preserved (Fig. 5b) in stalagmite

HS4 from Heshang cave in central China also revealed a relatively arid interval from 6.7 to 3.4 ka BP (Hu et al. 2008; Zhu et al. 2017). Therefore, it seems that mid-late Holocene paleohydrological evolution was asynchronous in the middle reaches of the Yangtze River of central China and in the Yellow River region of north China.

Tianchi Lake is located in the 'far-field' northwestern marginal region of the EASM, whereas the Dajiuhu peatland (Fig. 1a) is located in the 'core' monsoonal area of the EASM (Qian et al. 2007). Summer rainfall is the predominant contributor to the annual precipitation at both sites (Gao and Xie 2014). The northwards advance of the rainfall front resulting from an enhanced EASM intensity could result in increased precipitation in the marginal region of the EASM but decreased precipitation in the core monsoonal area of EASM (Ding et al. 2008; Rao et al. 2016). The occurrence of this contrasting spatial pattern of moisture conditions, with more frequent droughts in north China and more frequent floods in the mid-low Yangtze River valley during summer, has also been observed during the last few decades (Gemmer et al. 2004; Qian and Lin 2005; Zhai et al. 2005). It has been designated the "northern China drought and southern China flood" precipitation pattern (Zhou et al. 2009), and is also evident on millennial and centennial time scales (Chen et al. 2015b).

Previous workers have analyzed the main factors responsible for the asynchronous pattern of hydroclimatic variability between the marginal and core monsoonal area of EASM in China. For example, He et al. (2014) suggested that terrestrial temperature-induced evaporation changes and the extent of the Asian monsoonal front could potentially explain the out-of-phase pattern of hydrological

changes during the mid-Holocene. Chen et al. (2015a) emphasized that insolation forcing, especially the tropical ocean conditions might be responsible for the abrupt decline at 3.3 ka. Chen et al. (2015b) concluded that ENSO is one of the most important factors affecting the precipitation of monsoonal northern and central China on the centennial scale. Rao et al. (2016) emphasized the important influence of the west-east thermal gradient in the equatorial Pacific on the climate of monsoonal China. Zhu et al. (2017) concluded that a mid-Holocene reduction in ENSO intensity was related to a decrease in storm frequency in the middle reaches of Yangtze River between 6.7 and 3.4 ka BP. Finally, it is likely that the sea surface temperature (SST) anomaly in the equatorial Pacific during the mid-Holocene probably played a key role in facilitating the influence of ENSO on the asynchronous pattern of precipitation in the marginal and core monsoonal area of the EASM in China.

Conclusions

We have used the record of *n*-alkanes extracted from a lacustrine sediment core from Tianchi Lake on the Chinese Loess Plateau to reconstruct lake-level variations during the past 5.7 ka BP. P_{aq} values and C/N ratios through the sequence in general exhibit a gradually increasing trend through the past 5.7 ka BP, indicating an increasing (and more variable) abundance of submerged macrophytes in response to a falling lake level. Terrestrial plants dominated the record before 3.2 ka BP, and subsequently there was a shift to the dominance of submerged macrophytes. The predominance of

terrestrial plants agree with higher ACL, higher CPI, and lower P_{aq} values from 5.7-3.2 ka BP, whereas the dominance of submerged macrophytes resulted in lower ACL, lower CPI, and higher P_{aq} values after 3.2 ka BP. These changes indicate a relatively humid interval during 5.7-3.2 ka BP and a drier but more variable interval after 3.2 ka BP on the Chinese Loess Plateau. These findings are consistent with previous paleoclimatic reconstructions for the Loess Plateau which indicate a humid mid-Holocene. However, they are in disagreement with paleoclimatic records from central China, which indicate an arid mid-Holocene. Overall, this spatial pattern indicates that an enhanced intensity of monsoon rainfall delivered by the EASM during the mid-Holocene was an important factor in affecting paleohydrological changes in the region.

Acknowledgments

We thank Dr.Christopher Gallacher and Dr. Heiko Moossen for their training and help with laboratory analyses. This research was supported by grants from the National Science Foundation of China (NSFC Grants 41761044 and 41771208). We thank the China Scholarship Council (CSC) for funding a 20-month visit (File no. 2009618032) by Huiling Sun to work with Dr. James Bendle (now at the University of Birmingham) as a joint Ph.D. student (Lanzhou-Glasgow) at the G-MOL laboratory in Glasgow.

References

An CB, Feng ZD, Tang LY (2003) Evidence of a humid mid-Holocene in the western part of Chinese Loess Plateau. Chin Sci Bull 48: 2472-2479

Chen FH, Yu ZC, Yang ML, Ito E, Wang SM, Madsen DB, Huang XZ, Zhao Y, Sato T, Birks HJB, Boomer I, Chen JH, An CB, Wuennemann B (2008) Holocene moisture evolution in arid central Asia and its out-of-phase relationship with Asian monsoon history. Quat Sci Rev 27: 351-364

Chen FH, Xu QH, Chen JH, Birks HJB, Liu JB, Zhang SR, Jin LY, An CB, Telford RJ, Cao XY, Wang ZL, Zhang XJ, Selvaraj K, Lu HY, Li YC, Zheng Z, Wang HP, Zhou AF, Dong GH, Zhang JW, Huang XZ, Bloemendal J, Rao ZG (2015a) East Asian summer monsoon precipitation variability since the last deglaciation. Sci Rep 5: 11186

Chen JH, Chen FH, Feng S, Huang W, Liu JB, Zhou AF (2015b) Hydroclimatic changes in China and surroundings during the Medieval Climate Anomaly and Little Ice Age: spatial patterns and possible mechanisms. Quat Sci Rev 107: 98-111

Cheruvelil KS, Soranno PA (2008) Relationships between lake macrophyte cover and lake and landscape features. Aquat Bot 88: 219-227

Clift PD, Plumb RA (2008) The Asian monsoon: causes, history and effects. Cambridge University Press, Cambridge

Cranwell PA (1984) Lipid geochemistry of sediments from Upton Broad, a small productive lake. Org Geochem 7: 25-37

Ding YH, Wang ZY, Sun Y (2008) Inter-decadal variation of the summer precipitation in East China and its association with decreasing Asian summer monsoon. Part I: Observed

evidences. Int J Climatol 28: 1139-1161

Dong GH, Yang Y, Zhao Y, Zhou AF, Zhang XJ, Li XB, Chen FH (2012) Human settlement and human-environment interactions during the historical period in Zhuanglang County, western Loess Plateau, China. Quat Int 281: 78-83

Duarte CM, Kalf J (1986) Littoral slope as a predictor of the maximum biomass of submerged macrophyte communities. Limnol Oceanogr 31: 1072-1080

Ficken KJ, Li B, Swain DL, Eglinton G (2000) An *n*-alkane proxy for the sedimentary input of submerged/floating freshwater aquatic macrophytes. Org Geochem 31: 745-749

Gao L, Hou JZ, Toney J, MacDonald DL, Huang YS (2011) Mathematical modeling of the aquatic macrophyte inputs of mid-chain n-alkyl lipids to lake sediments: implications for interpreting compound specific hydrogen isotopic records. Geochim Cosmochim Acta 75: 3781-3791

Gao T, Xie LA (2014) Study on progress of the trends and physical causes of extreme precipitation in China during the last 50 years. Adv Earth Sci 29: 577-589

Gemmer M, Becker S, Jiang T (2004) Observed monthly precipitation trends in China 1951-2002. Theor Appl Clim 77: 39-45

He YX, Zheng YW, Pan AD, Zhao C, Sun YY, Song M, Zheng Z, Liu ZH (2014) Biomarker-based reconstructions of Holocene lake-level changes at Lake Gahai on the northeastern Tibetan Plateau. The Holocene 24: 405-412

He YX, Zhao C, Zheng Z, Liu ZH, Wang N, Li J, Cheddadi R (2015) Peatland evolution and associated environmental changes in central China over the past 40,000 years. Quat Res 84: 255-261

Huang XY, Xue JT, Wang XX, Meyers PA, Huang JH, Xie SC (2013) Paleoclimate influence on early diagenesis of plant triterpenes in the Dajiuhu peatland, central China. Geochim Cosmochim Acta 123: 106-119

Hudon C (1997) Impact of water level fluctuations on St. Lawrence River aquatic vegetation. Can J Fish Aquat Sci 54: 2853-2865

Hudon C, Lalonde S, Gagnon P (2000) Ranking the effects of site exposure, plant growth form, water depth, and transparency on aquatic plant biomass. Can J Fish Aquat Sci 57: 31-42

Kawamura K (1995) Land-derived lipid class compounds in the deep-sea sediments and marine aerosols from North Pacific. In: Biogeochemical Processes and Ocean Flux in the Western Pacific. Terra Scientific Publishing Company, Tokyo, pp 31-51

Kawamura K, Ishimura Y, Yamazaki K (2003) Four years' observations of terrestrial lipid class compounds in marine aerosols from the western North Pacific. Global Biogeochem Cy 17: 3-1-3-19

Lamb AL, Leng MJ, Mohammed MU, Lamb HF (2004) Holocene climate and vegetation change in the Main Ethiopian Rift Valley, inferred from the composition (C/N and $\delta^{13}C$) of lacustrine organic matter. Quat Sci Rev 23: 881-891

Ling Y, Zheng MP, Sun Q, Dai XQ (2017) Last deglacial climatic variability in Tibetan Plateau as inferred from *n*-alkanes in a sediment core from Lake Zabuye. Quat Int 454: 15-24

Liu FG, Feng ZD (2012) A dramatic climatic transition at ~4,000 cal. yr BP and its cultural responses in Chinese cultural domains. The Holocene 22: 1181-1197

Liu H, Liu WG (2016) *n*-Alkane distributions and concentrations in algae, submerged plants and terrestrial plants from the Qinghai-Tibetan Plateau. Org Geochem 99: 10-22

Liu JB, Chen JH, Zhang XJ, Li Y, Rao ZG, Chen FH (2015) Holocene East Asian summer monsoon records in northern China and their inconsistency with Chinese stalagmite $\delta^{18}O$ records. Earth-Sci Rev 148: 194-208

Liu WG, Yang H, Wang HY, An ZS, Wang Z, Leng Q (2015) Carbon isotope composition of long chain leaf wax *n*-alkanes in lake sediments: A dual indicator of paleoenvironment in the Qinghai-Tibet Plateau. Org Geochem 83: 190-201

Lu HY, Yi SW, Liu ZY, Mason JA, Jiang DB, Cheng J, Stevens T, Xu ZW, Zhang EL, Jin LY (2013) Variation of East Asian monsoon precipitation during the past 21 ky and potential CO_2 forcing. Geology 41: 1023-1026

Marzi R, Torkelson BE, Olson RK (1993) A revised carbon preference index. Org Geochem 20: 1303-1306

Meyers PA (1997) Organic geochemical proxies of paleoceanographic, paleolimnologic, and paleoclimatic processes. Org Geochem 27: 213-250

Meyers PA, Ishiwatari R (1993) Lacustrine organic geochemistry - an overview of indicators of organic matter sources and diagenesis in lake sediments. Org Geochem 20: 867-900

Middelboe AL, Markager S (1997) Depth limits and minimum light requirements of freshwater macrophytes. Freshw Biol 37: 553-568

Nichols JE, Booth RK, Jackson ST, Pendall EG, Huang YS (2006) Paleohydrologic reconstruction based on *n*-alkane distributions in ombrotrophic peat. Org Geochem 37: 1505-1513

Poynter J, Eglinton G (1990) Molecular composition of three sediments from hole 717c: The Bengal fan. In: Proceedings of the Ocean Drilling Program: Scientific results, 116: pp.

155-161

Pu, Y, Zhang HC, Lei GL, Chang FQ, Yang MS, Zhang WX, Lei YB, Yang LQ, Pang YZ (2010) Climate variability recorded by *n*-alkanes of paleolake sediment in Qaidam Basin on the northeast Tibetan Plateau in late MIS3. China Earth Sci: 53: 624-631 (In Chinese)

Qian W, Lin X (2005) Regional trends in recent precipitation indices in China. Meteorol Atmos Phys 90: 193-207

Qian WH, Lin X, Zhu YF, Xu Y, Fu JL (2007) Climatic regime shift and decadal anomalous events in China. Clim Change 84: 167-189

Qiang MR, Song L, Chen FH, Li MZ, Liu XX, Wang Q (2013) A 16 ka lake-level record inferred from macrofossils in a sediment core from Genggahai Lake, northeastern Qinghai-Tibetan Plateau (China). J Paleolimnol 49: 575-590

Rao ZG, Jia GD, Li YX, Chen JH, Xu QH, Chen FH (2016) Asynchronous evolution of the isotopic composition and amount of precipitation in north China during the Holocene revealed by a record of compound-specific carbon and hydrogen isotopes of long-chain *n*-alkanes from an alpine lake. Earth Planet Sci Lett 446: 68-76

Reimer PJ, Baillie MGL, Bard E, Bayliss A, Beck JW, Bertrand CJH, Blackwell PG, Buck CE, Burr GS, Cutler KB, Damon PE, Edwards RL, Fairbanks RG, Friedrich M, Guilderson TP, Hogg AG, Hughen KA, Kromer B, McCormac FG, Manning SW, Ramsey CB, Reimer RW, Remmele S, Southon JR, Stuiver M, Talamo S, Taylor FW, van der Plicht, J, Weyhenmeyer CE, (2004) IntCal04 terrestrial radiocarbon age calibration, 0-26 cal kyr BP. Radiocarbon 46: 1029-1058

Rielley G, Collier RJ, Jones DM, Eglinton G (1991) The biogeochemistry of Ellesmere Lake,

UK-I: source correlation of leaf wax inputs to the sedimentary lipid record. Org Geochem 17: 901-912

Sachse D, Radke J, Gleixner G (2006) δD values of individual *n*-alkanes from terrestrial plants along a climatic gradient - Implications for the sedimentary biomarker record. Org Geochem 37: 469-483

Seki O, Harada N, Sato M, Kawamura K, Ijiri A, Nakatsuka T (2012) Assessment for paleoclimatic utility of terrestrial biomarker records in the Okhotsk Sea sediments. Deep Sea Research Part II: Topical Studies in Oceanography 61: 85-92

Street JH, Anderson RS, Rosenbauer RJ, Paytan A (2013) *n*-Alkane evidence for the onset of wetter conditions in the Sierra Nevada, California (USA) at the mid-late Holocene transition, ~ 3.0 ka. Quat Res 79: 14-23

Vogts A, Moossen H, Rommerskirchen F, Rullkötter J (2009) Distribution patterns and stable carbon isotopic composition of alkanes and alkan-1-ols from plant waxes of African rain forest and savanna C_3 species. Org Geochem 40: 1037-1054

Wagner T, Falter CM (2002) Response of an aquatic macrophyte community to fluctuating water levels in an oligotrophic lake. Lake Reservoir Manag 18: 52-65

Wang HP, Chen JH, Zhang XJ, Chen FH (2014) Palaeosol development in the Chinese Loess Plateau as an indicator of the strength of the East Asian summer monsoon: Evidence for a mid-Holocene maximum. Quat Int 334: 155-164

Wang SW, Huang JB, Wen XY, Zhu JH (2008) Evidence and modeling study of droughts in China during 4-2 ka BP. Chin Sci Bull 53: 2215-2221

Xie SC, Evershed RP, Huang XY, Zhu ZM, Pancost RD, Meyers PA, Gong LF, Hu CY,

Huang JH, Zhang SH, Gu YS, Zhu JY (2013) Concordant monsoon-driven postglacial hydrological changes in peat and stalagmite records and their impacts on prehistoric cultures in central China. Geology 41: 827-830

Xue JT, Li JJ, Dang XY, Meyers PA, Huang XY (2017) Paleohydrological changes over the last 4,000 years in the middle and lower reaches of the Yangtze River: Evidence from particle size and *n*-alkanes from Longgan Lake. The Holocene 27: 1318-1324

Zhai PM, Zhang XB, Wan H, Pan XH (2005) Trends in total precipitation and frequency of daily precipitation extremes over China. J Climate 18: 1096-1108

Zhao Y, Chen FH, Zhou AF, Yu ZC, Zhang K (2010) Vegetation history, climate change and human activities over the last 6200 years on the Liupan Mountains in the southwestern Loess Plateau in central China. Palaeogeogr Palaeoclimatol Palaeoecol 293: 197-205

Zhou TJ, Gong DY, Li J, Li B (2009) Detecting and understanding the multi-decadal variability of the East Asian Summer Monsoon-recent progress and state of affairs. Meteorol Z 18: 455-467

Zhou WJ, Douglas JD, Stephen CP, Timothy AJ, Li XQ, Minze S, An ZS, Eiji M, Dong GR (1996) Variability of monsoon climate in East Asia at the end of the last glaciation. Quat Res 46: 219-229

Zhu ZM, Feinberg JM, Xie SC, Bourne MD, Huang CJ, Hu CY, Cheng H (2017) Holocene ENSO-related cyclic storms recorded by magnetic minerals in speleothems of central China. Proc Natl Acad Sci 114: 852-857

Figure captions

Fig. 1. (a) Location of Tianchi Lake in North China. Solid dots represent the study area and other study sites referenced in the text. The map shows the correlation coefficients between summer precipitation in China and summer monsoon intensity from 1951-2000 (Wang et al. 2008), (b) schematic representation of the bathymetry of Tianchi Lake (depths in m), (c) laminated structure of the sediment cores from Tianchi Lake, (d) photo of submerged macrophytes in the shallow area of Tianchi Lake

Fig. 2. Age-depth model for core GSB07-1 from Tianchi Lake

Fig. 3. Histogram of the molecular distributions of *n*-alkanes from (a) modern terrestrial plants, (b) modern emergent macrophytes, (c) modern submerged macrophytes, (d) surface lake sediments and (e) surface soils from around Tianchi Lake. Only odd carbon number distributions are shown for the *n*-alkanes

Fig. 4. Time series of sedimentary parameters for core GSB07-1 from Tianchi Lake over the past 5.7 ka BP. (a) P_{aq} values based-on *n*-alkanes, (b) *n*-alkane ACL, (c) *n*-alkane CPI, (d) C/N ratios

Fig. 5. Comparison of regional paleohydrological records. (a) Heshang cave speleothem $\delta^{18}O$ records (Hu et al. 2008), (b) the flux of soil-derived magnetic minerals ($IRM_{soft\text{-}flux}$) preserved in stalagmite HS4 (Zhu et al. 2017), (c) hopanoids

flux in Dajiuhu peatland (Xie et al. 2013), (d) P_{aq} values based-on *n*-alkanes in Tianchi Lake, (e) pollen-based reconstruction of mean annual precipitation (MAP) from Tianchi Lake (Chen et al. 2015a), (f) pollen-based reconstruction of mean annual precipitation (MAP) from Gonghai Lake (Chen et al. 2015a), (g) July Insolation at 30 °N (Berger and Loutre 1991)

Table 1. AMS radiocarbon dates of core GSA07-1 in Tianchi Lake and the chronology of core GSB07-1 based on depth calibration with core GSA07-1

Core GSA07-1						Core GSB07-1	
Depth (cm)	Material dated	$\delta^{13}C$ (‰ VPDB)	^{14}C date (yr BP)	Error (±yr)	Calibrated age (Cal yr BP-2σ range)	Calibrated depth (cm)	Calibrated age (Cal yr BP)
162	Tree leaves	-29.0	680	30	619±56	174	662±21
183	Tree leaves	-26.9	855	35	740±47	193	776±27
221	Tree leaves	-21.1	1080	35	963±35	228	1009±33
260	Tree leaves	-11.6	1255	30	1169±42	240	1088±23
302	Tree leaves	-18.7	1440	45	1378±37	257	1192±14
383	Tree leaves	-21.0	1775	30	1793±30	366	1768±58
436	Tree leaves	-24.3	2060	30	2089±42	443	2217±82
489	Tree leaves	-23.1	2355	30	2398±52	509	2633±37
510	Tree leaves	-17.6	2520	35	2537±49	526	2719±26
518	Tree leaves	-12.7	2585	40	2580±52	532	2754±25
554	Tree leaves	-26.3	2415	35	2789±51	545	2830±25
570	Tree leaves	-25.4	2830	30	2898±45	554	2891±30
600	Tree leaves	-16.6	2895	45	3097±51	593	3130±43
660	Tree leaves	-19.7	3300	30	3520±43	658	3538±38
701	Tree leaves	-30.3	3400	30	3793±36	700	3810±19
732	Tree leaves	-24.4	3720	35	4002±33	730	4012±28
751	Tree leaves	-20.2	3935	35	4149±45	754	4174±21
815	Tree leaves	-14.7	4100	40	4547±33	816	4540±29
848	Tree leaves	-19.5	4230	35	4726±33	838	4653±28
893	Tree leaves	-18.3	4400	40	4937±41	882	4899±33
966	Tree leaves	-16.3	4495	40	5277±33	957	5290±25
1014	Tree leaves	-25.6	4820	40	5513±32	992	5497±26
1049	Tree leaves	-27.1	4970	35	5689±34	1023	5673±33
1086	Tree leaves	-25.4	5030	35	5870±33		
1114	Tree leaves	-24.4	5440	70	6038±41		

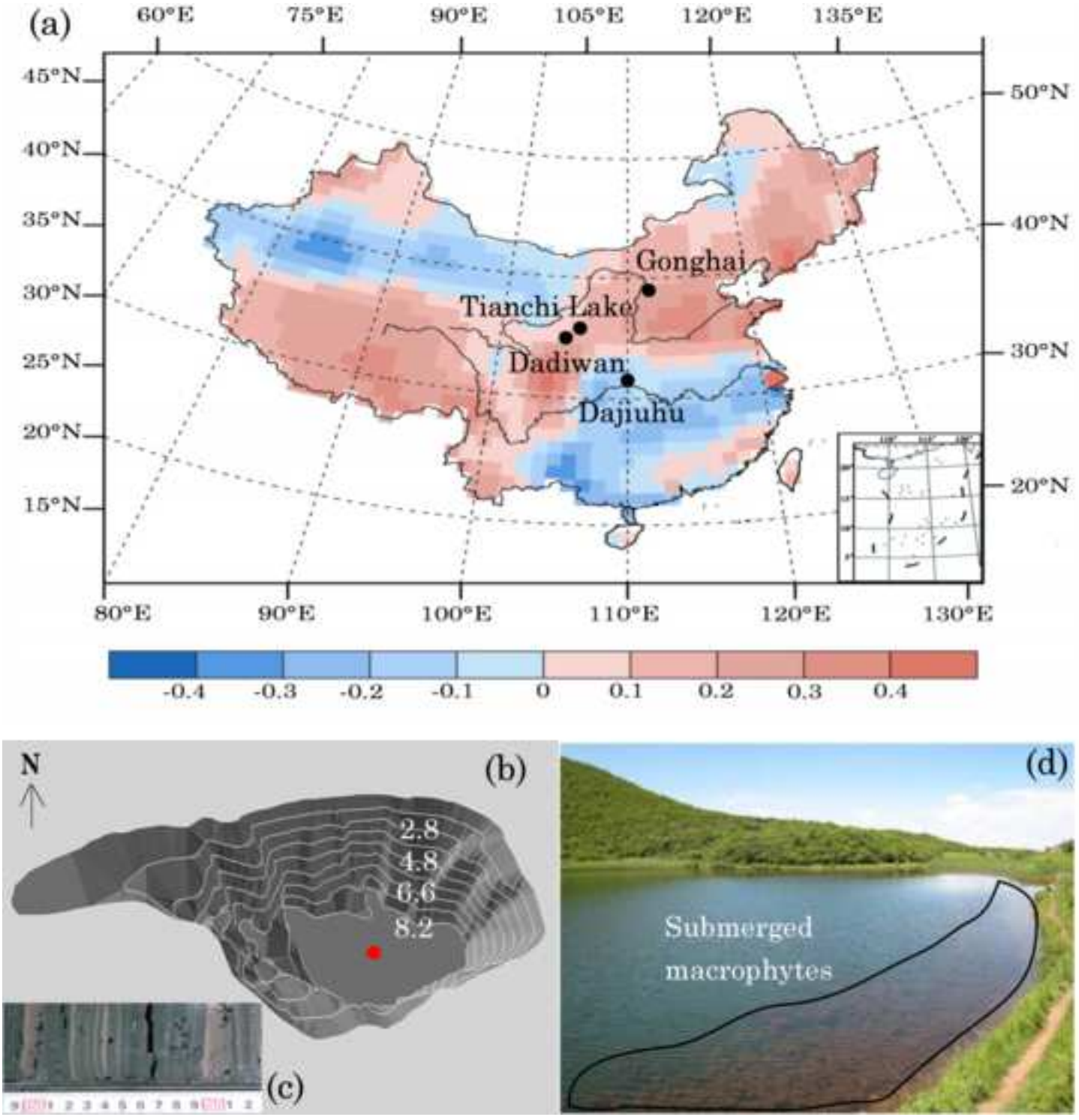

fig2

Click here to download Figure Fig.2-GSB-new.pdf

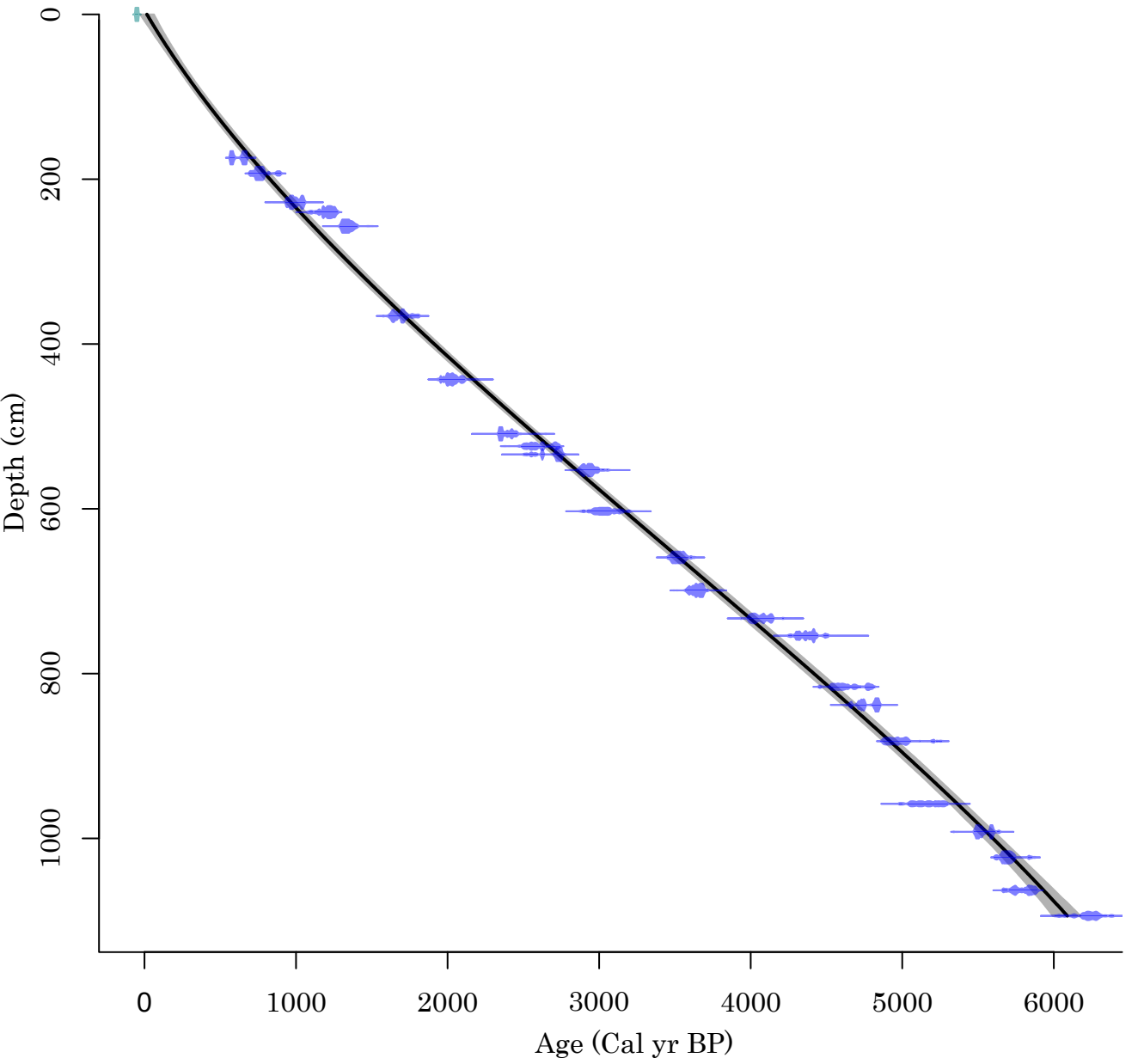

Figure3

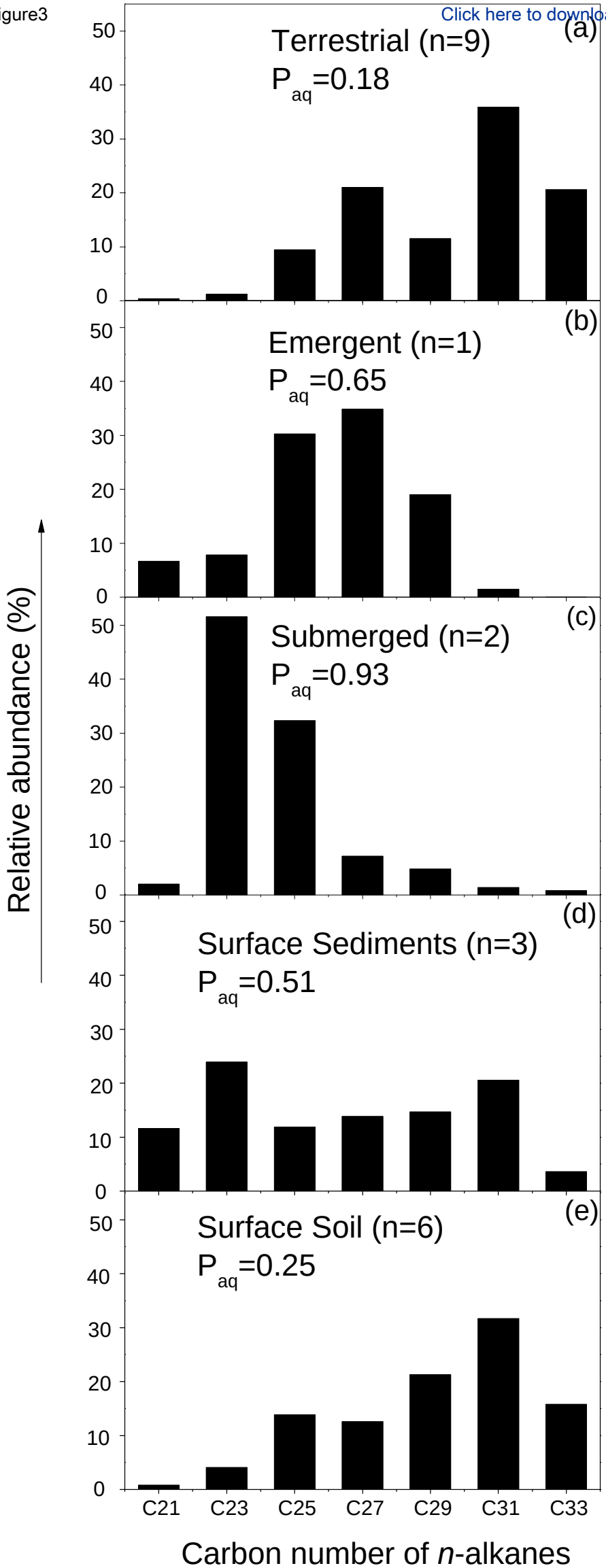

Figure4

Click here to download Figure Fig.4..pdf

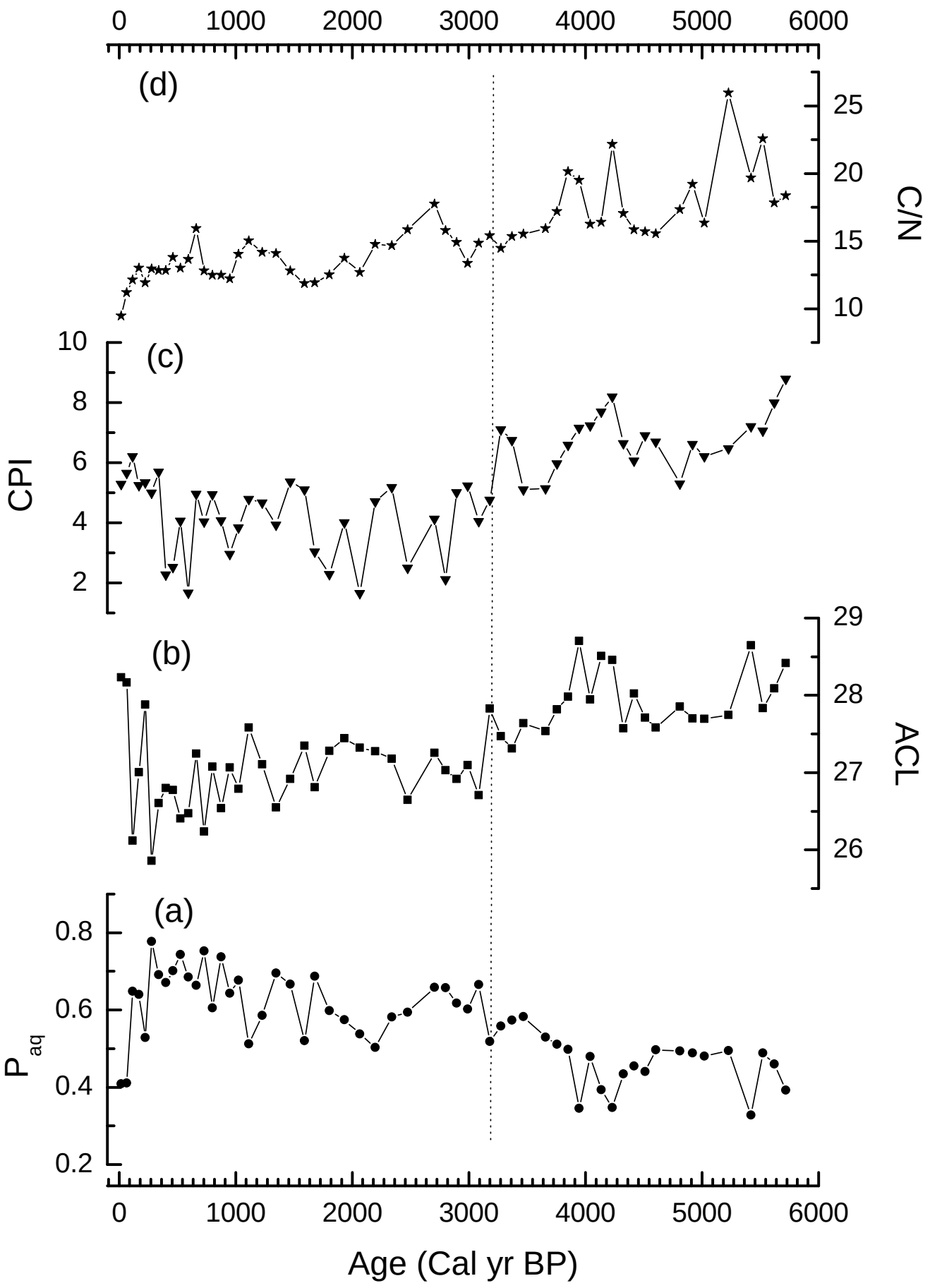

Figure5

Click here to download Figure Fig.5.2018-03-08.tif

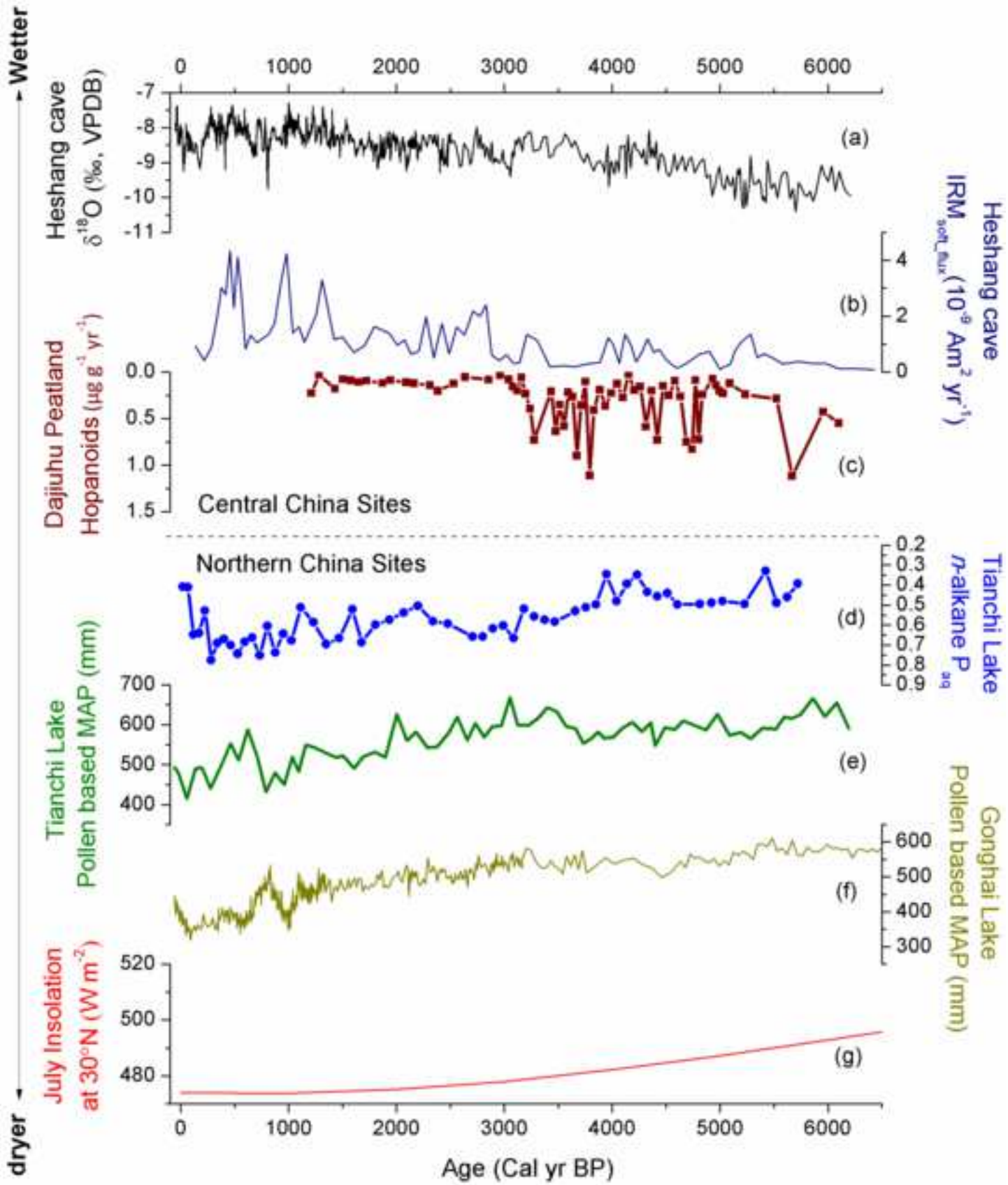

Table 1

Core GSA07-1						Core GSB07-1	
Depth (cm)	Material dated	δ13C (‰ VPDB)	14C date (yr BP)	Error (±yr)	Calibrated age (Cal yr BP-2σ range)	Calibrated depth (cm)	Calibrated age (Cal yr BP)
162	Tree leaves	-29.0	680	30	619±56	174	662±21
183	Tree leaves	-26.9	855	35	740±47	193	776±27
221	Tree leaves	-21.1	1080	35	963±35	228	1009±33
260	Tree leaves	-11.6	1255	30	1169±42	240	1088±23
302	Tree leaves	-18.7	1440	45	1378±37	257	1192±14
383	Tree leaves	-21.0	1775	30	1793±30	366	1768±58
436	Tree leaves	-24.3	2060	30	2089±42	443	2217±82
489	Tree leaves	-23.1	2355	30	2398±52	509	2633±37
510	Tree leaves	-17.6	2520	35	2537±49	526	2719±26
518	Tree leaves	-12.7	2585	40	2580±52	532	2754±25
554	Tree leaves	-26.3	2415	35	2789±51	545	2830±25
570	Tree leaves	-25.4	2830	30	2898±45	554	2891±30
600	Tree leaves	-16.6	2895	45	3097±51	593	3130±43
660	Tree leaves	-19.7	3300	30	3520±43	658	3538±38
701	Tree leaves	-30.3	3400	30	3793±36	700	3810±19
732	Tree leaves	-24.4	3720	35	4002±33	730	4012±28
751	Tree leaves	-20.2	3935	35	4149±45	754	4174±21
815	Tree leaves	-14.7	4100	40	4547±33	816	4540±29
848	Tree leaves	-19.5	4230	35	4726±33	838	4653±28
893	Tree leaves	-18.3	4400	40	4937±41	882	4899±33
966	Tree leaves	-16.3	4495	40	5277±33	957	5290±25
1014	Tree leaves	-25.6	4820	40	5513±32	992	5497±26
1049	Tree leaves	-27.1	4970	35	5689±34	1023	5673±33
1086	Tree leaves	-25.4	5030	35	5870±33	1060	5871±35
1114	Tree leaves	-24.4	5440	70	6038±41	1094	6078±58